ACS Biomaterials SCIENCE & ENGINEERING

pubs.acs.org/journal/abseba Article

Xeno-Free Bioreactor Culture of Human Mesenchymal Stromal Cells on Chemically Defined Microcarriers

John D. Krutty, Kevin Koesser, Stephen Schwartz, Junsu Yun, William L. Murphy, and Padma Gopalan*

Cite This: *ACS Biomater. Sci. Eng.* 2021, 7, 617−625 Read Online

ACCESS | Metrics & More | Article Recommendations | Supporting Information

ABSTRACT: Human mesenchymal stromal cells (hMSC), also called mesenchymal stem cells, are adult cells that have demonstrated their potential in therapeutic applications, highlighted by their ability to differentiate down different lineages, modulate the immune system, and produce biologics. There is a pressing need for scalable culture systems for hMSC due to the large number of cells needed for clinical applications. Most current methods for expanding hMSC fail to provide a reproducible cell product in clinically required cell numbers without the use of serum-containing media or harsh enzymes. In this work, we apply a tailorable, thin, synthetic polymer coating—poly(poly(ethylene glycol) methyl ether methacrylate-*ran*-vinyl dimethyl azlactone-*ran*-glycidyl methacrylate) (P(PEGMEMA-*r*-VDM-*r*-GMA), PVG)—to the surface of commercially available polystyrene (PS) microcarriers to create chemically defined three-dimensional (3D) surfaces for large-scale cell expansion. These chemically defined microcarriers provide a reproducible surface that does not rely on the adsorption of xenogeneic serum proteins to mediate cell adhesion, enabling their use in xeno-free culture systems. Specifically, this work demonstrates the improved adhesion of hMSC to coated microcarriers over PS microcarriers in xeno-free media and describes their use in a readily scalable, bioreactor-based culture system. Additionally, these surfaces resist the adsorption of media-borne and cell-produced proteins, which result in integrin-mediated cell adhesion throughout the culture period. This feature allows the cells to be efficiently passaged from the microcarrier using a chemical chelating agent (ethylenediaminetetraacetic acid (EDTA)) in the absence of cleavage enzymes, an improvement over other microcarrier products in the field. Bioreactor culture of hMSC on these microcarriers enabled the production of hMSC over 4 days from a scalable, xeno-free environment.

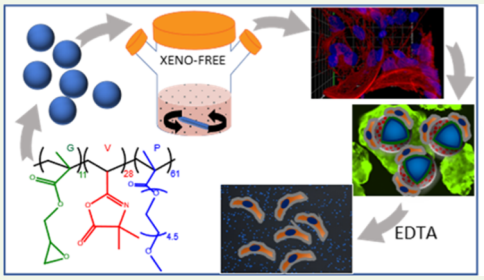

KEYWORDS: *mesenchymal stromal cell, bioreactor, biomanufacturing, MSC*

INTRODUCTION

Human mesenchymal stromal cells (hMSCs), also called mesenchymal stem cells, are a relevant cell type for many therapeutic and research applications due to their immunosuppressive potential,[1−3] ability to differentiate down multiple lineages,[4−9] and production of biologics.[10−12] In the last 15 years, these cells have been the subject of over 900 clinical trials, with over 100 trials conducted per year since 2015 (clinicaltrials.gov). As the demand for hMSC and other cell types continues to rise, there is a pressing need for reproducible, cost-effective manufacturing methods to produce these cells. Some innovations have been made to facilitate the production of cells at scale, including large tissue culture flasks, cell stack plates, bioreactors, and microcarriers.[13] Microcarriers are typically solid, 100−300 μm diameter beads that enable cell adhesion before being cultured in suspension in a stirred bioreactor. The constant mixing in a microcarrier-containing bioreactor introduces enhanced gas and nutrient exchange[14] and therefore can be scaled up to large vessels and to manufacture large numbers of cells. They provide a higher surface area for cell growth and require less media, culture material, and labor and as such are one of the leading target systems for cell manufacturing.[15−17] Microcarriers are commonly made of polymers, including poly(hydroxyethyl methacrylate) (PHEMA),[18] polystyrene (PS),[19−21] polyacrylamide (PA),[22,23] poly(L-lactic acid) (PLLA),[24] and poly(lactic-*co*-glycolic acid) (PLGA),[25] and stimuli-responsive materials[26] including poly(*N*-isopropylacrylamide) (pNIPAAm),[27] and they are often coated with charged molecules, peptides (e.g., Corning Synthemax, CellBIND), or proteins (e.g., collagen, gelatin, Cultispher-S) that facilitate cell adhesion. Examples of commercially available microcarriers include Corning (PS uncoated or Synthemax coated), dextran-based Cytodex I, II, and III (GE Healthcare), Sigma-Solohill (collagen- or recombinant protein-coated), and Cultispher (Percell Biolytica AB).

Typical cell production methods are dependent on xenogeneic solid and soluble components such as fetal bovine

Received: May 5, 2020
Accepted: December 24, 2020
Published: January 14, 2021

https://dx.doi.org/10.1021/acsbiomaterials.0c00663
ACS Biomater. Sci. Eng. 2021, 7, 617−625

serum (FBS), collagen, Matrigel, and others.[28,29] As research into cell-based therapeutics advances, there is a growing body of evidence suggesting that there are drawbacks to the inclusion of xenogeneic components. Animal-derived products suffer from high cost, issues with production, and batch-to-batch variations,[28,30] which can introduce variability into cell culture and have negative effects on the cell as the end product.[31,32] Additionally, xenogeneic components may be incorporated into the cell itself, which can induce antigenicity and an associated immune response from the recipient of a cell-based therapeutic and in some extreme cases has resulted in anaphylaxis.[33,34] Synthetic cell culture materials have been developed in two-dimensional (2D)[35−40] and three-dimensional (3D)[41−45] to culture stem cells and direct stem cell fate, but in most cases, these materials are not amenable to scale up for cell production at scale. Recent publications have described the use of human serum as an additive to enable hMSC culture on microcarriers in xeno-free media.[46,47] While this recent work was able to achieve hMSC adhesion to uncoated (human serum-incubated) microcarriers in xeno-free media, we focus on the use of existing xeno-free media formulations with the polymer-coated microcarriers. In this work, we develop on our previously reported[48−50] poly(poly(ethylene glycol) methyl ether methacrylate-*ran*-vinyl dimethyl azlactone-*ran*-glycidyl methacrylate) (P(PEGMEMA-*r*-VDM-*r*-GMA), (PVG))-coated microcarrier culture system[51] to enable microcarrier culture in scalable bioreactors in media free of xenogeneic components (xeno-free media). We first demonstrate the potential of the PVG to coat a wide range of cell culture materials, through its successful application to 96-well and 384-well plates with circular and rectangular wells, respectively. We also demonstrate that by optimizing the concentration of the poly-L-lysine (PLL) anchoring layer in the sequential anchoring method the coating can resist the nonspecific adhesion (adhesion that is not mediated via a defined ligand) of hMSC. These PVG-coated microcarriers are then applied to hMSC culture in xeno-free media and in bioreactors that can be readily scaled to create therapeutically relevant numbers of hMSC without exposing them to xenogeneic components. Additionally, the chemically defined surface prevents the nonspecific adsorption of serum and cell-produced extracellular matrix (ECM) proteins. This reduction in ECM protein adsorption controls the adhesion of hMSC through the integrin-binding RGD peptide. We show that this integrin-specific adhesion enables efficient, enzyme-free, ethylenediaminetetraacetic acid (EDTA)-based passaging of hMSC, further reducing the cost of materials needed for cell culture over the state-of-the-art commercially available coated microcarriers. Importantly, hMSC cultured on PVG-coated microcarriers in xeno-free, bioreactor conditions retained their immunopotency and multipotent differentiation capacity, showing that this culture system has the potential to be used for therapeutic cell production while maintaining the required critical quality attributes.

EXPERIMENTAL SECTION

PVG Copolymer Synthesis. PVG copolymer was synthesized using reversible addition−fragmentation chain transfer anionic polymerization (RAFT), by copolymerization of poly(ethylene glycol) methyl ether methacrylate (PEGMEMA), glycidyl methacrylate (GMA), and vinyl dimethyl azlactone (VDM) according to previously reported procedures.[51] The resultant polymer P(PEGMEMA-*r*-VDM-*r*-GMA) was dissolved and stored in tetrahydrofuran (THF). Gel permeation chromatography (GPC) yielded a M_n = 47 000 and a dispersity of 2.1. Proton nuclear magnetic resonance spectroscopy showed that the final concentration of the copolymer was 61% PEGMEMA, 29% VDM, and 10% GMA.

Optimization of PVG Coating on Multiwell Plates. 96-well and 384-well tissue culture polystyrene (TCPS) plates were coated with PVG copolymer via the sequential anchoring process described in Krutty et al.[51] Briefly, TCPS plates were incubated in 70 000−150 000 kDa poly-L-lysine (Sigma-Aldrich, Milwaukee, WI) solutions in water at concentrations of either 0.01 or 0.05 wt %, depending on the condition being tested, for 1 h. PLL adsorbs to polystyrene largely though hydrophobic interactions, and its use is common in cell culture applications.[52−54] Each well was rinsed 2× with 300 μL of dH_2O and 1× with 300 μL of 200 proof EtOH. Finally, wells were filled with 10−50 μL of 10 mg mL^{-1} PVG solution in EtOH and allowed to react overnight.

PVG Coating of Microcarriers. Untreated polystyrene microcarriers with a diameter of 125−212 μm (Corning, Corning, NY) were weighed and incubated in 0.05 wt % 70 000−150 000 Da poly-L-lysine for 1 h. Microcarriers were then washed twice with dH_2O and once with EtOH. Microcarriers were placed in a 10 mg mL^{-1} solution of PVG polymer in EtOH and allowed to react overnight. Microcarriers at this state were stored in EtOH at −20 °C for up to 1 month.

Peptide Immobilization. PVG-coated surfaces were washed twice with phosphate-buffered saline (PBS) and reacted with Cys-Gly-Gly-Gly-Arg-Gly-Asp-Ser-Pro (CGGGRGDSP, "RGD"), Cys-Gly-Gly-Gly-Arg-Asp-Gly-Ser-Pro (CGGGRDGSP, "scramble") peptides (Genscript). TCPS plates and microcarriers were incubated in 1 mM peptide solutions in 1× phosphate-buffered saline (PBS) (Fisher Scientific) for 1 h at room temperature according to the previously established procedure.[49,50] The coated surfaces were then rinsed twice with PBS and sanitized in 70% ethanol for 30 min before use in cell culture.

hMSC Culture. *Serum-Containing Medium.* hMSC (Lonza PT-2501 Lot # 0000684888) were cultured in minimum essential medium-α (αMEM) modification (Corning, Corning, MA) plus 10% fetal bovine serum (FBS) (Gibco, Cat. #16000-044, Dublin, Ireland). Cells were thawed from LN2 storage and seeded onto T175 TCPS plates at 2800 cells cm^{-2}. Cells were incubated at 37 °C and 5% CO_2 and manipulated under sterile conditions. Media was changed after 24 h, then every 2−3 days. Cells were passaged at 70−80% confluence using 5 mL of trypsin (Fisher/Hyclone, SH30236.02) at 37 °C and 5% CO_2 for 5 min. After 5 min, adherent cells were loosened using gentle agitation of the plate

Xeno-Free Medium. hMSC (RoosterBio, XF RoosterKit-hBM Lot 164) were cultured in RoosterNourish MSC-XF xeno-free media (Roosterbio, Frederick, MD). Cells were thawed from LN2 storage and seeded onto T175 TCPS plates at 2800 cells cm^{-2}. Cells were incubated at 37 °C and 5% CO_2 and manipulated under sterile conditions. Media was changed after 24 h, then every 2−3 days. Cells were passaged at 70−80% confluence using 5 mL of TrypLE Select Enzyme (Invitrogen, Carlsbad CA) at 37 °C and 5% CO_2 for 5 min. After 5 min, adherent cells were loosened using gentle agitation of the plate.

hMSC Adhesion on Multiwell Plates. To evaluate hMSC attachment to PVG + RGD surfaces, passage 4−6 hMSC were seeded (10 000 cells cm^{-2}) in αMEM + 10% FBS on PS, PLL-coated, PVG-coated, RGD functionalized, and scramble functionalized TCPS plates, prepared as previously described. After 24 h, the cells were fixed, stained for nuclei and actin cytoskeleton, and imaged.

Microcarrier Suspension Culture in 24-Well Plates. To study hMSC attachment and expansion on PVG + RGD microcarrier surfaces, hMSC were grown for up to a week in either αMEM + 10% FBS or RoosterNourish MSC-XF media. Passage 4−6 cells were seeded in 500 μL of media onto 10 cm^2 of microcarriers in an ultra-low-adhesion 24-well plates (Corning). A cell seeding density of 10 000 hMSC cm^{-2} was used with each of the following surface functionalization: PS, PVG-coated, PVG + RGD peptide (PVG + RDG), or PVG + scramble peptide. At desired time points (1, 2, 4, and 7 days), cells were either fixed and stained or lysed, and total DNA was quantified using a CyQUANT Cell Proliferation Assay Kit, per kit instructions.

Microcarrier Suspension Culture in Stirred Flask Bioreactors. Seven hundred fifteen milligrams of PVG + RGD microcarriers were

https://dx.doi.org/10.1021/acsbiomaterials.0c00663
ACS Biomater. Sci. Eng. 2021, 7, 617−625

added to 30 mL of αMEM + 10% FBS or RoosterNourish media in a 125 mL, nontreated, PS disposable spinner flask (Corning). Typically, 1.5×10^6 cells were seeded onto the microcarriers, and the working volume was brought to 67 mL (approximately one half of the bioreactor's capacity). A static incubation period of 4−12 h was used to encourage cell adhesion before starting the stirring process. For all cell expansion and cell phenotype quantification data, a 12 h static incubation period was used. The bioreactor was then placed on a magnetic stir plate in the incubator (37 °C, 5% CO_2) and agitated at a rate of 60 rpm. One half volume media changes (approx. 33 mL) were performed after 96 h.

Fluorescent Imaging. Live hMSC were stained with 1 μM Calcein AM (Thermo Fisher). For fluorescent imaging of fixed cells, hMSC were washed with 1× PBS and fixed in 10% buffered formalin solution for 20−30 min. Cells were then permeabilized with 0.1% Triton X-100 (MP Biomedicals, Aurora, OH) in 1× PBS for 20 min. Cells were washed twice with PBS and blocked using 1% bovine serum albumin (BSA) (Fisher Scientific). Cells were stained for actin cytoskeleton using Alexa-Fluor 647 Phalloidin (Thermo Fisher) and for nuclei using 4′,6-diamidine-2′-phenylindole dihydrochloride (DAPI) (Sigma-Aldrich) or Hoechst 33342 for 30 min each, washing in between with PBS. Cells were imaged on an inverted microscope with DAPI, fluorescein isothiocyanate (FITC), and far red filter cube sets.

Cell Passaging and Quantification. hMSC nuclei were counted to determine cell number, seeding efficiency, and passaging efficiency.

hMSC Passaging. hMSC were passaged using Versene, a 1× ethylenediaminetetraacetic acid (EDTA) solution (Invitrogen). EDTA lifts cells from surfaces through the chelation of Ca^{2+} and Mg^{2+} ions, which are an important component of integrin receptor binding.

hMSC Seeding Efficiency and Quantification. Representative samples were removed from the bioreactor in 3 × 1 mL samples on day 1. hMSC nuclei were stained using 2 μM Hoechst 33342 (Thermo Fisher), a cell membrane permeable fluorescent stain. Samples were allowed to settle for 30 min before being imaged in phase and fluorescence, and adherent cells were quantified using eq 1

$$\text{seeding efficiency} = \frac{\text{microcarrier adjacent nuclei}}{\text{total nuclei}} \times 100\% \quad (1)$$

where microcarrier adjacent nuclei are defined as nuclei belonging to cells that are attached to microcarriers as visualized in the fluorescent microscope images, and total nuclei are defined as nuclei belonging to cells attached to the microcarriers and the nuclei from cells not attached to microcarrier. The nuclei were counted from images using NIS Elements software to identify and catalogue individual nuclei.

hMSC Passaging and Passaging Efficiency. hMSC were lifted from the microcarrier surface using either TrypLE or EDTA. Microcarriers were removed from the bioreactor in 1 mL of samples, rinsed with PBS, and incubated in the passaging solution for 4 min at 37 °C and 5% CO_2, agitated through gentle pipetting, and returned to the incubator for another 4 min. Samples were stained using Hoechst 33342, then placed in a multiwell plate and allowed to settle for 30 min before imaging. Samples were imaged in phase and fluorescence, and passaging efficiency was quantified using eq 2

$$\text{passaging efficiency} = \frac{\text{unassociated nuclei}}{(\text{unassociated nuclei} + \text{microcarrier adjacent nuclei})} \times 100\% \quad (2)$$

where unassociated nuclei are defined as those nuclei belonging to cells that are not adhered to the surface of a microcarrier as visualized in the phase microscope images.

hMSC Expansion on Microcarriers. Cells were grown on microcarriers in a 125 mL stirred flask bioreactor (Corning) as described previously and passaged as described earlier in this section. Microcarriers were then separated from the nonadherent cells using a cell strainer (Corning Falcon) with a pore size of 100 μm. Samples were stained using Hoechst 33342, then placed in a multiwell plate and allowed to settle for 30 min before imaging. Samples were imaged in phase and fluorescence, where the number of nuclei was used as a proxy for total cell number.

hMSC Differentiation and Cell Function. To evaluate differentiation capacity after expansion on coated microcarriers, hMSC were differentiated to osteoblasts and adipocytes based on established protocols. For differentiation, hMSC were seeded at 5000 cells cm^{-2} on collagen-coated plates (Corning, Corning, NY) in 10% FBS in αMEM and permitted to grow to confluence for 3 days. Osteogenic (OS) medium and adipogenic induction medium (AIM) were prepared. OS medium consisted of 10% FBS in αMEM with 0.1 μM dexamethasone, 10 mM β glycerol phosphate, and 50 μM ascorbic acid 2-phosphate. AIM consisted of 10% FBS in Dulbecco's modification of Eagle's medium (DMEM) high glucose with penicillin (100 U mL^{-1})/streptomycin (100 μg mL^{-1}), 1 μM dexamethasone, 10 μg mL^{-1} insulin, and 500 μM isomethyl isobutyl xanthine (IBMX). Media was changed every 3−4 days, and analysis was performed after 21 days of differentiation. As negative controls, cells were grown for 21 days in 10% FBS in αMEM.

Alizarin Red S stained mineral deposits from osteoblasts, and Oil Red O stained lipid droplets in adipocytes. To perform staining, cells were fixed in 10% buffered formalin solution and incubated Alizarin Red S (40 mM, pH 4.1−4.3) and washed three times with water or Oil Red O working solution for 20 min and washed with water until washings were clear. Working Oil Red O solution was prepared by mixing three parts stock Oil Red O solution (3 mg mL^{-1} in 99% isopropanol) with two parts distilled water and filtering with a 0.2 μm syringe filter.

hMSC were stained for β-galactosidase activity using the Senescence Cell Histochemical Staining Kit (Sigma). Cells were washed with 1× PBS and fixed using 10% buffered formalin. Cells were then stained according to manufacturer's specifications, immersed in the staining solution at 37 °C for 12 h.

hMSC immunopotency was measured using an L-kynurenine assay. hMSC were harvested after 4 days of culture on PVG + RGD microcarriers and seeded at a cell density of 40 000 cells cm^{-2} in xeno-free media. At 24 h, the growth media was changed and supplemented with 10 ng mL^{-1} interferon-γ (IFN-γ) (R&D Systems, Minneapolis, MN). Cells were incubated with IFN-γ-containing media for 24 h, at which point 150 μL of spent media was collected and stored at −80 °C for up to 1 month before testing. Cells were fixed with 10% buffered formalin, stained using Hoechst 33342, and imaged. Nuclei were counted using NIS Elements binary thresholding software to get an accurate cell count of the number of cells per well. Spent media was thawed, and proteins were precipitated from each sample using 50 μL of trichloroacetic acid (Sigma-Aldrich) per 100 μL of sample. Precipitates were removed by 5 min centrifugation at 950*g*. Seventy-five microliters of supernatant was then added to a clear-bottom 96-well plate and mixed with 75 μL of Ehrlich's reagent (Sigma-Aldrich). The absorbance of light at a wavelength of 490 nm was taken using an automatic plate reader. L-Kynurenine concentration was determined by a linear regression of concentration compared to a standard curve, which was produced in triplicate.

Statistical Analysis. Experiments were carried out and repeated a total of two to three trials, with $n = 3-4$ replicates per trial. Statistics were analyzed for this work using the Microsoft Excel Analysis ToolPak Add-in. Except where noted, a one-way analysis of variance (ANOVA) was conducted to determine significance, as there are multiple groups with one independent variable. A post hoc Tukey's test was then used to determine the significance between groups.

RESULTS

Previously, we reported[51] a sequential anchoring method for the stable application of PVG onto planar and three-dimensional surfaces. In this method, a commercially available cell culture material (0.01% poly-L-lysine in water) was used to improve cell adhesion. PLL acts as an anchoring layer for PVG; hence, the uniformity of this layer also influences the uniformity of the PVG coating and subsequent cell adhesion. We tested different

https://dx.doi.org/10.1021/acsbiomaterials.0c00663
ACS Biomater. Sci. Eng. 2021, 7, 617−625

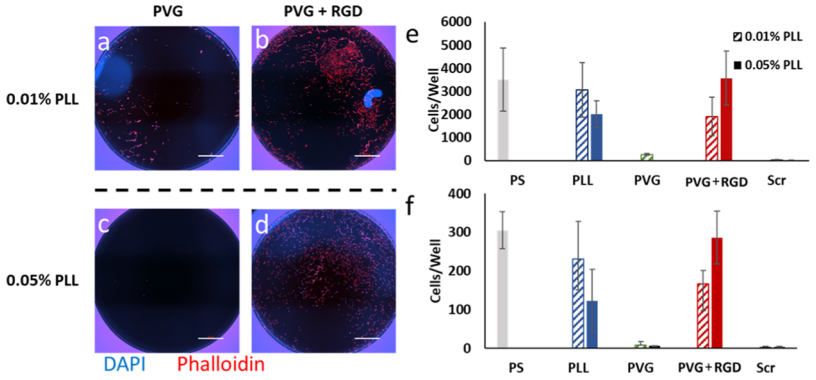

Figure 1. Increasing the PLL content during the sequential anchoring process improves the application of PVG copolymer to multiwell plates. (a, b) 0.01% and (c, d) 0.05% PLL solutions were used to create PVG-coated 96-well plates. (a, c) Unfunctionalized PVG-coated plates reduce nonspecific cell adhesion. (b, d) RGD functionalization (PVG + RGD) restores cell adhesion to PVG-coated plates. Quantification of cell number in both (e) 96-well and (f) 384-well plates shows that using 0.05% PLL solutions improved resistance to nonspecific adhesion in PVG-coated wells and improved adhesion in PVG + RGD wells. Scale bar = 1000 μm.

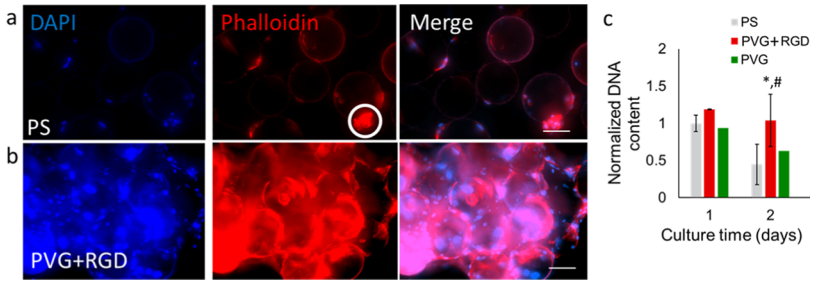

Figure 2. hMSC adhesion in xeno-free media is enhanced on PVG + RGD-coated microcarriers over uncoated PS microcarriers. (a) Poor adhesion to PS microcarriers is shown by few adhered cells and rounded cell morphology (circled). (b) Large aggregate of hMSC and PVG + RGD microcarriers indicates strong adhesion. Blue = DAPI; red = rhodamine phalloidin. Scale bar = 100 μm. (c) DNA quantification of hMSC on microcarriers over time. The reduction in DNA content between days 1 and 2 on PS microcarriers indicates the removal of nonadherent cells during media changes. * Denotes $p < 0.05$ by one-way ANOVA with respect to PS microcarriers day 2; # denotes $p < 0.05$ with respect to PVG.

concentrations of the PLL anchoring layer in 96-well and 384-well tissue culture polystyrene plates (Figures 1 and S1).

At a PLL concentration of 0.05 wt %, the PVG coating was most effective at resisting the nonspecific adhesion of hMSC (Figure 1a,c) and enabled integrin-mediated cell adhesion after functionalization with the RGD peptide (Figure 1b,d). The effectiveness of each coating was quantified using cell number/well as a measure of the well's adhesivity (Figure 1e,f). This improved sequential anchoring method was used for all subsequent experiments on microcarriers in xeno-free media.

hMSC Adhesion to PVG-Coated Microcarriers in Xeno-Free Media. Uncoated PS microcarriers were used as a control in xeno-free media. The DNA content on PS microcarriers decreased after changing the media at 24 h, similar to the decrease seen on PVG-coated microcarriers (Figure 2).

Unadhered cells were removed during a media change between days 1 and 2; therefore, the decrease in DNA content is indicative of poor adhesion to the bare PS and unfunctionalized PVG surfaces. Few cells seeded onto PS microcarriers adhered, and those that did adopted a rounded morphology indicating a poorly adhesive surface (Figures 2a and S2). The extent of hMSC spreading on PVG + RGD microcarriers is further evident in the confocal micrographs shown in Movie S1. We quantified the cell seeding efficiency of 77% for hMSC seeded on PVG + RGD microcarriers using eq 1. These cell seeding results show that PVG + RGD microcarriers may enable scalable hMSC culture in xeno-free media.

hMSC Expansion and Enzyme-Free Passaging in Xeno-Free Media. hMSC were cultured in xeno-free media on PVG + RGD microcarriers in a 125 mL stirred flask bioreactor (Figure 3) to evaluate their potential for scale up to industrial processes. hMSC were seeded onto microcarriers according to the manufacturers' recommendations in xeno-free media and allowed to attach for 12 h in static conditions, before being cultured in suspension for 7 days. One milliliter of samples were taken at days 1, 2, 4, and 7, cells passaged from the surface using EDTA, and nuclei stained using Hoechst 33342. To track the expansion of hMSC over time, the cells were imaged and nuclei counted (Figures 4 and S3).

Cell number increased up to day 4, at which point large aggregates of microcarriers and cells reduced expansion rate (Figures 4e and S3). This is similar to the expansion pattern observed in serum-containing media.[51] hMSC cultured on PVG + RGD microcarriers maintained a well-spread morphology, adhering to and following the curvature of the microcarriers (Figure 4f and Movie S1). One of the advantages of PVG + RGD-coated surfaces over traditional cell culture surfaces is the ability to passage using nonenzymatic, chemical chelating agents such as EDTA. This process is gentle on the cells, contains no animal products, and has been shown on planar substrates to preserve the cell culture surface and patterned peptides.[49] To quantify the efficacy of EDTA passaging from PVG + RGD microcarriers, 1 mL of samples of the microcarriers in suspension in a bioreactor were harvested on days 2, 4, and 7.

https://dx.doi.org/10.1021/acsbiomaterials.0c00663
ACS Biomater. Sci. Eng. 2021, 7, 617−625

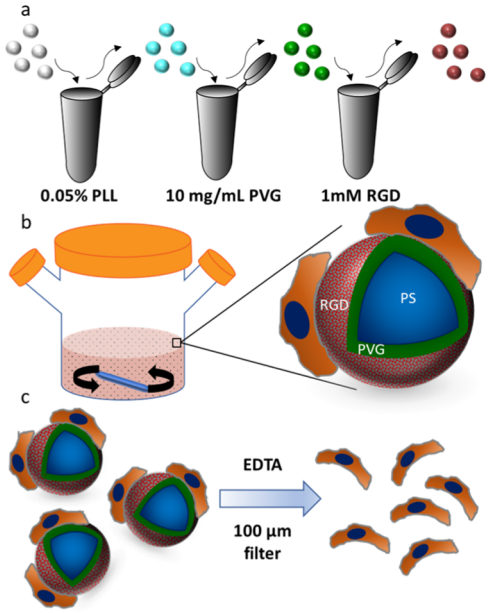

Figure 3. Xeno-free, scalable hMSC culture on microcarriers. (a) PS microcarriers are functionalized using a sequential anchoring process of PLL adsorption, followed by PVG copolymer anchoring, and RGD functionalization. (b) hMSC are then cultured in xeno-free media in a stirred flask bioreactor for up to 7 days. (c) After 7 days, hMSC are passaged using EDTA and separated from the microcarriers using a cell strainer with a pore size of 100 μm.

hMSC were separated from the microcarriers using EDTA and stained for nuclei using Hoechst 33342 (Figure 5).

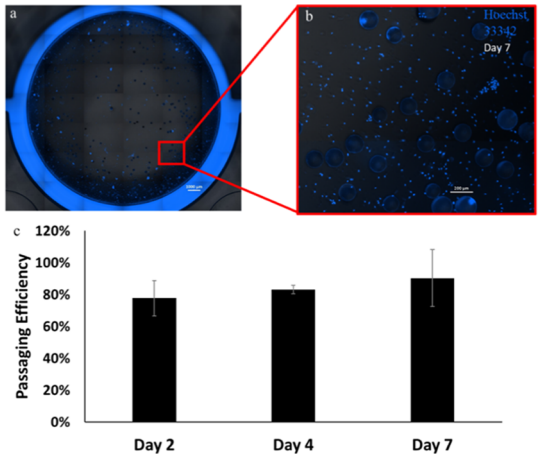

Figure 5. EDTA passaging remains effective throughout a 7-day culture period. (a, b) Fluorescent micrographs of hMSC grown on PVG + RGD microcarriers cultured in Roosterbio MSC-XF xeno-free media and passaged using EDTA. (c) Quantification of passaging efficiency (percentage of cells removed from microcarriers by EDTA) was defined as the percentage of total nuclei that were detached from microcarriers after EDTA exposure (eq 2). Blue = DAPI, scale bars (a) 1000 and (b) 200 μm.

Passaging efficiency, determined using eq 2, shows that 77−85% of cells were singularized and separated from the surface using EDTA, and this efficiency did not decrease as aggregates became larger over time (Figure 5b). As a comparison, for the cells cultured on the commercially available Corning Synthemax microcarriers, EDTA alone was not sufficient to separate the cells from the microcarriers, leaving large aggregates intact (Figure S4).

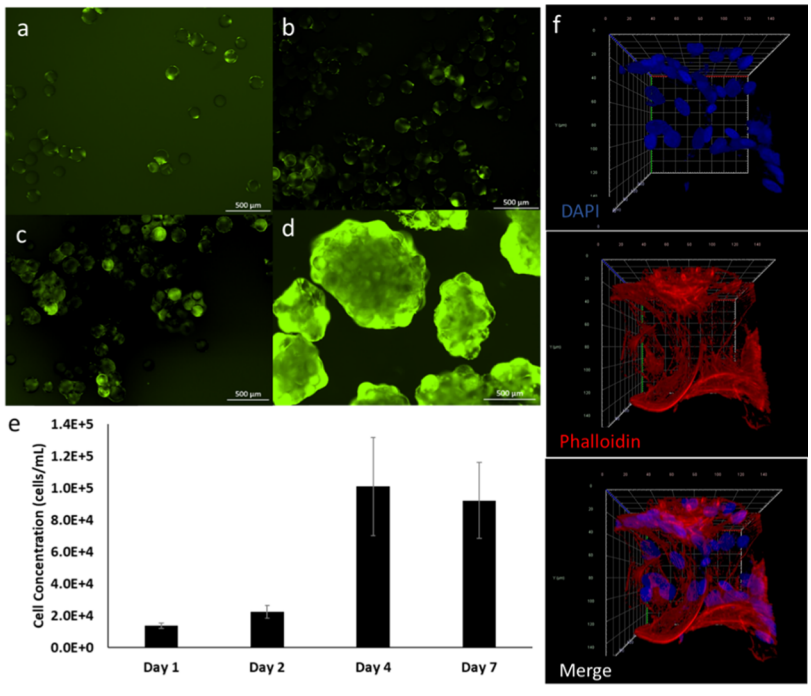

Figure 4. hMSC expansion on PVG + RGD microcarriers suspended in 125 mL bioreactors in Roosterbio-XF xeno-free media: hMSC were cultured for 1, 2, 4, or 7 days ((a)−(d), respectively), at which point a 1 mL of sample was removed from the bioreactor. Live cells were stained using Calcein AM and imaged (scale bar = 500 μm). In separate samples, cells were passaged using EDTA, separated from the microcarriers, and stained using Hoechst 33342. Nuclei were counted and used to obtain a measure of the cell concentration in the bioreactor (e). Confocal images of cells after 4 days of microcarrier culture show well-spread morphology and the formation of cell and microcarrier aggregates (f). Scale grid = 150 μm.

https://dx.doi.org/10.1021/acsbiomaterials.0c00663
ACS Biomater. Sci. Eng. 2021, 7, 617−625

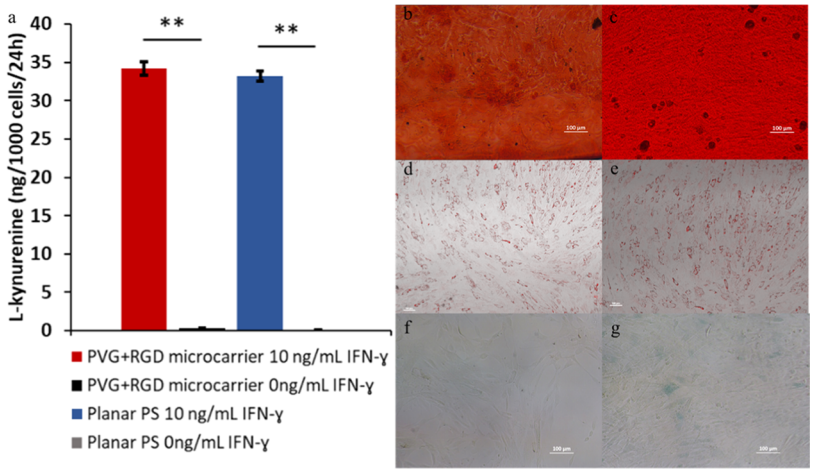

Figure 6. hMSC function after culture on PVG + RGD microcarriers in xeno-free media in a bioreactor. (a) hMSC cultured on PVG + RGD microcarriers retain their immunosuppressive potential as measured by L-kynurenine production. $^{**}p < 0.01$. hMSC stained positively for mineral deposition when differentiated down the osteogenic lineage following bioreactor (b) or planar (c) culture. Cells differentiated down the adipogenic lineage stained positively for lipid deposits by Oil Red O after bioreactor (d) or planar (e) culture. hMSC did not show an apparent increase in senescence-associated β-galactosidase (blue) after bioreactor culture (f) when compared to cells cultured on planar surfaces (g). Scale bar = 100 μm.

hMSC Differentiation and Immunosuppression Post-microcarrier Culture. hMSC are an ideal cell type for scale up and manufacturing due to their multipotency and immunosuppressive potential. To evaluate the potency of hMSC grown in xeno-free media on PVG + RGD microcarriers, cells cultured in the bioreactor were differentiated down the adipogenic and osteogenic lineages. Cells were harvested from the microcarriers and seeded on collagen-I coated plates and differentiated for 21 days and stained with the Oil Red O or Alizarin Red S, for adipogenic differentiation and osteogenic differentiation, respectively (Figure 6).

Cells grown on PVG + RGD microcarriers retained their immunomodulatory potential when stimulated with IFN-γ as demonstrated by an L-kynurenine assay. The production of L-kynurenine by hMSC is an important regulator in immune cell function and is mediated through the enzyme indolamine dioxygenase (IDO).[55,56] hMSC also demonstrated the capacity to differentiate down both the adipogenic and osteogenic lineages, as measured by lipid and mineral deposition, respectively. Additionally, hMSC cultured on microcarriers in a bioreactor did not show signs of senescence as measured by β-galactosidase staining (Figure 6).

DISCUSSION

hMSC continue to be an important cell type for their therapeutic potential, even as the desired trait has expanded to include immunosuppressive behavior in addition to differentiation potential.[57−59] Most recently, hMSC attracted interest after demonstrating promise to dampen the cytokine storm and acute respiratory distress syndrome that can result from SARS-CoV2 infection.[60] To address the issues inherent to large-scale cell culture, we have demonstrated the capability for the bioreactor culture of hMSC on a tailorable, chemically defined surface in xeno-free culture media.

To maximize cell seeding efficiency on 3D-coated microcarriers, the uniformity of the PVG coating was improved by increasing the concentration of the adsorbed PLL (Figures 1 and S1). The unfunctionalized, PVG-coated wells prepared with a higher concentration of PLL reduced nonspecific cell adhesion. This is a significant advance over previous iterations of the sequential anchoring process, as it ensures that the adhesion to the surface is mediated solely through the RGD peptide, which enables enzyme-free, EDTA-based passaging from these surfaces.

The improved sequential coating method also increases the potential of these surfaces to be tailored to specific applications outside of cell adhesion. In Figure S5, we demonstrated tailoring these microcarriers with a vascular endothelial growth factor (VEGF) binding peptide (VBP). These PVG + VBP microcarriers are capable of reducing the amount of soluble VEGF detectable in the supernatant media by enzyme-linked immunosorbent assay (ELISA). Other growth factor-binding materials have been shown to modify cellular response to that growth factor.[61,62] PVG-coated microcarriers have the potential to similarly reduce the need for soluble growth factors in the culture media, a large component of the media cost.

PVG + RGD-coated microcarriers have the potential to improve the efficiency and cost-effectiveness of large-scale cell culture. As demonstrated in Figure 3, uncoated PS microcarriers are incapable of enabling cell adhesion and growth in xeno-free media. The few cells that do attach to PS surfaces adopt a rounded morphology, indicative of poor adhesion. This lack of adhesion is likely due to the absence of fetal bovine serum (FBS) or other xenogeneically derived serum components that enables cell adhesion through their adsorption to PS surface, similar to the process that enables adhesion to TCPS plates.[54,63] Therefore, microcarrier culture of hMSC in xeno-free media relies on the use of coated microcarriers. The only synthetic, RGD-based coating for microcarriers in the market now is Corning Synthemax II, which enables cell adhesion and growth in xeno-free media. However, currently there are no chemically defined or tailorable coatings for microcarriers that can be purchased through commercial sources. Importantly, the PVG + RGD microcarriers allow efficient passaging with EDTA, due to the integrin-specific adhesion to the chemically defined surface, which is not possible on Synthemax II-coated microcarriers. On Synthemax II-coated microcarriers, exposure to EDTA fails to break up the aggregates of cells and microcarriers, making it impossible to isolate and purify the cells for use (Figure S2). The ability to passage cells using EDTA removes the need for harsh,

https://dx.doi.org/10.1021/acsbiomaterials.0c00663
ACS Biomater. Sci. Eng. 2021, 7, 617−625

enzymatic passaging methods. Additionally, the 77% passaging efficiency from PVG + RGD microcarriers using EDTA meets the critical detachment yield for single-use bioreactor systems to surpass planar surfaces in cost-effectiveness for the smallest batch sizes.[16]

hMSC cultured on PVG + RGD microcarriers in a 125 mL bioreactor in xeno-free media showed adhesion and growth over 4 days and maintained a population doubling time between 24 and 26 h. This paper demonstrates proof of concept for using a chemically defined microcarrier functionalized for integrin-mediated cell adhesion in xeno-free media. However, the number of cells produced and cost-effectiveness of the batch production can be improved through the scale up to larger bioreactors and optimization of seeding density and culture conditions, as the reported size scale for which single-use bioreactors are the most cost efficient is for batch sizes of at least 500 M−1 B cells.[16,64] Additional factors such as microcarrier density, cell seeding density, agitation rate, and media changes will all need to be optimized to create a cost-effective culture system.

Importantly, hMSC cultured on PVG + RGD microcarriers in xeno-free media cells retained their potential for differentiation down the adipogenic and osteogenic lineages as shown by lipid and mineral deposition, respectively. Furthermore, the immunosuppressive potential of these cells was not significantly altered when compared to traditional planar culture at the same cell density. In addition, as a result of microcarrier culture or the coating, no measurable increase in cellular senescence was observed, suggesting that as a result of increased shear forces, the rate of aging of these cells does not increase. Finally, the ability to scale production of hMSC in xeno-free media coupled with the potential reduced material cost of functionalized, PVG-coated microcarriers represents an important improvement over the state of the art in the field.

■ ASSOCIATED CONTENT

Supporting Information

The Supporting Information is available free of charge at https://pubs.acs.org/doi/10.1021/acsbiomaterials.0c00663.

Micrographs of hMSCs grown on PVG-coated wells, hMSCs seeded to bare PS microcarriers, and 11 day bioreactor culture of hMSC in xeno-free and serum-containing media (PDF)

Confocal micrographs showing the extent of hMSC spreading on PVG + RGD microcarriers (Movie S1) (AVI)

■ AUTHOR INFORMATION

Corresponding Author

Padma Gopalan − *Department of Materials Science and Engineering and Department of Biomedical Engineering, University of Wisconsin−Madison, Madison, Wisconsin 53706, United States; Department of Chemistry, University of Wisconsin−Madison, Madison, Wisconsin 53706, United States;* orcid.org/0000-0002-1955-640X; Email: pgopalan@wisc.edu

Authors

John D. Krutty − *Department of Materials Science and Engineering, University of Wisconsin−Madison, Madison, Wisconsin 53706, United States;* orcid.org/0000-0001-7104-5239

Kevin Koesser − *Department of Biomedical Engineering, University of Wisconsin−Madison, Madison, Wisconsin 53706, United States*

Stephen Schwartz − *Department of Biomedical Engineering, University of Wisconsin−Madison, Madison, Wisconsin 53706, United States*

Junsu Yun − *Department of Materials Science and Engineering, University of Wisconsin−Madison, Madison, Wisconsin 53706, United States*

William L. Murphy − *Department of Materials Science and Engineering, Department of Biomedical Engineering, and Department of Orthopedics and Rehabilitation, University of Wisconsin−Madison, Madison, Wisconsin 53706, United States*

Complete contact information is available at: https://pubs.acs.org/10.1021/acsbiomaterials.0c00663

Author Contributions

The manuscript was written through the contributions of all authors. All authors have given approval to the final version of the manuscript.

Notes

The authors declare no competing financial interest.

■ ACKNOWLEDGMENTS

This work was completed with funding support from the NSF DMR 1709179 and the Wisconsin Alumni Research Foundation Accelerator program.

■ ABBREVIATIONS

hMSC, human mesenchymal stromal cell; PVG, poly(poly-(ethylene glycol)-*ran*-vinyl dimethyl azlactone-*ran*-glycidyl methacrylate; RGD, Arg-Gly-Asp peptide

■ REFERENCES

(1) Follin, B.; Juhl, M.; Cohen, S.; Pedersen, A. E.; Kastrup, J.; Ekblond, A. Increased Paracrine Immunomodulatory Potential of Mesenchymal Stromal Cells in Three-Dimensional Culture. *Tissue Eng., Part B* **2016**, *22*, 322−329.

(2) Le Blanc, K.; Davies, L. C. Mesenchymal stromal cells and the innate immune response. *Immunol. Lett.* **2015**, *168*, 140−146.

(3) Chen, X.; Armstrong, M. A.; Li, G. Mesenchymal stem cells in immunoregulation. *Immunol. Cell Biol.* **2006**, *84*, 413−421.

(4) Pittenger, M. F.; Mackay, A. M.; Beck, S. C.; Jaiswal, R. K.; Douglas, R.; Mosca, J. D.; Moorman, M. A.; Simonetti, D. W.; Craig, S.; Marshak, D. R. Multilineage Potential of Adult Human Mesenchymal Stem Cells. *Science* **1999**, *284*, 143−147.

(5) Shen, X.; Pan, B.; Zhou, H.; Liu, L.; Lv, T.; Zhu, J.; Huang, X.; Tian, J. Differentiation of mesenchymal stem cells into cardiomyocytes is regulated by miRNA-1-2 via WNT signaling pathway. *J. Biomed. Sci.* **2017**, *24*, No. 29.

(6) Singh, A.; Singh, A.; Sen, D. Mesenchymal stem cells in cardiac regeneration: a detailed progress report of the last 6 years (2010−2015). *Stem Cell Res. Ther.* **2016**, *7*, No. 82.

(7) Silva, G. V.; Litovsky, S.; Assad, J. A. R.; Sousa, A. L. S.; Martin, B. J.; Vela, D.; Coulter, S. C.; Lin, J.; Ober, J.; Vaughn, W. K.; Branco, R. V. C.; Oliveira, E. M.; He, R.; Geng, Y.-J.; Willerson, J. T.; Perin, E. C. Mesenchymal Stem Cells Differentiate into an Endothelial Phenotype, Enhance Vascular Density, and Improve Heart Function in a Canine Chronic Ischemia Model. *Circulation* **2005**, *111*, 150−156.

(8) Augello, A.; De Bari, C. The Regulation of Differentiation in Mesenchymal Stem Cells. *Hum. Gene Ther.* **2010**, *21*, 1226−1238.

(9) Chamberlain, G.; Fox, J.; Ashton, B.; Middleton, J. Concise review: mesenchymal stem cells: their phenotype, differentiation

capacity, immunological features, and potential for homing. *Stem Cells* **2007**, *25*, 2739−2749.
(10) Baek, G.; Choi, H.; Kim, Y.; Lee, H.-C.; Choi, C. Mesenchymal Stem Cell-Derived Extracellular Vesicles as Therapeutics and as a Drug Delivery Platform. *Stem Cells Transl. Med.* **2019**, *8*, 880−886.
(11) Caplan, A. I.; Dennis, J. E. Mesenchymal stem cells as trophic mediators. *J. Cell. Biochem.* **2006**, *98*, 1076−1084.
(12) Rani, S.; Ryan, A. E.; Griffin, M. D.; Ritter, T. Mesenchymal Stem Cell-derived Extracellular Vesicles: Toward Cell-free Therapeutic Applications. *Mol. Ther.* **2015**, *23*, 812−823.
(13) Panchalingam, K. M.; Jung, S.; Rosenberg, L.; Behie, L. A. Bioprocessing strategies for the large-scale production of human mesenchymal stem cells: a review. *Stem Cell Res. Ther.* **2015**, *6*, No. 225.
(14) Malda, J.; Frondoza, C. G. Microcarriers in the engineering of cartilage and bone. *Trends Biotechnol.* **2006**, *24*, 299−304.
(15) Rowley, J.; Abraham, E.; Campbell, A.; Brandwein, H.; Oh, S. Meeting lot-size challenges of manufacturing adherent cells for therapy. *BioProcess Int.* **2012**, *10*, 16−22.
(16) Pereira Chilima, T. D.; Moncaubeig, F.; Farid, S. S. Impact of allogeneic stem cell manufacturing decisions on cost of goods, process robustness and reimbursement. *Biochem. Eng. J.* **2018**, *137*, 132−151.
(17) dos Santos, F.; Campbell, A.; Fernandes-Platzgummer, A.; Andrade, P. Z.; Gimble, J. M.; Wen, Y.; Boucher, S.; Vemuri, M. C.; da Silva, C. L.; Cabral, J. M. S. A xenogeneic-free bioreactor system for the clinical-scale expansion of human mesenchymal stem/stromal cells. *Biotechnol. Bioeng.* **2014**, *111*, 1116−1127.
(18) Ayhan, H.; Kozluca, A.; Pişkin, E.; Gurhan, I. Attachment of 3T3 and MDBK Cells onto PHEMA-Based Microbeads and their Biologically Modified Forms. *J. Bioact. Compat. Polym.* **1999**, *14*, 17−30.
(19) Heathman, T. R.; Glyn, V. A.; Picken, A.; Rafiq, Q. A.; Coopman, K.; Nienow, A. W.; Kara, B.; Hewitt, C. J. Expansion, harvest and cryopreservation of human mesenchymal stem cells in a serum-free microcarrier process. *Biotechnol. Bioeng.* **2015**, *112*, 1696−1707.
(20) Szczypka, M.; Splan, D.; Woolls, H.; Brandwein, H. Single-use bioreactors and microcarriers. *BioProcess Int.* **2014**, *12*, 54−64.
(21) Kehoe, D.; DiLeo, A.; Simler, J.; Ball, A.; Schnitzler, A. C. Scale-up of Human Mesenchymal Stem Cells on Microcarriers in Suspension in a Single-use Bioreactor. *BioPharm Int.* **2012**, *25*, 28.
(22) Reuveny, S.; Mizrahi, A.; Kotler, M.; Freeman, A. Mammalian cell propagation on derivatized polyacrylamide microcarriers. *Dev. Biol. Stand.* **1983**, *55*, 11−23.
(23) Reuveny, S.; Mizrahi, A.; Kotler, M.; Freeman, A. New Microcarriers for Culturing Mammalian Cells. *Ann. N. Y. Acad. Sci.* **1983**, *413*, 413−415.
(24) Tan, H.; Wu, J.; Huang, D.; Gao, C. The Design of Biodegradable Microcarriers for Induced Cell Aggregation. *Macromol. Biosci.* **2010**, *10*, 156−163.
(25) Chun, K. W.; Yoo, H. S.; Yoon, J. J.; Park, T. G. Biodegradable PLGA Microcarriers for Injectable Delivery of Chondrocytes: Effect of Surface Modification on Cell Attachment and Function. *Biotechnol. Prog.* **2004**, *20*, 1797−1801.
(26) Brun-Graeppi, A. K. A. S.; Richard, C.; Bessodes, M.; Scherman, D.; Merten, O.-W. Cell microcarriers and microcapsules of stimuli-responsive polymers. *J. Controlled Release* **2011**, *149*, 209−224.
(27) Kim, M. R.; Jeong, J. H.; Park, T. G. Swelling Induced Detachment of Chondrocytes Using RGD-Modified Poly(N-isopropylacrylamide) Hydrogel Beads. *Biotechnol. Prog.* **2002**, *18*, 495−500.
(28) Xiaoyang, Z.; Haven, B.; S, H. W.; Farah, F.; Michael, M.; Erno, P. Proteomic Analysis for the Assessment of Different Lots of Fetal Bovine Serum as a Raw Material for Cell Culture. Part IV. Application of Proteomics to the Manufacture of Biological Drugs. *Biotechnol. Prog.* **2006**, *22*, 1294−1300.
(29) Tekkatte, C.; Gunasingh, G. P.; Cherian, K. M.; Sankaranarayanan, K. "Humanized" Stem Cell Culture Techniques: The Animal Serum Controversy. *Stem Cells Int.* **2011**, *2011*, No. 504723.
(30) Cheng, C. W.; Solorio, L. D.; Alsberg, E. Decellularized tissue and cell-derived extracellular matrices as scaffolds for orthopaedic tissue engineering. *Biotechnol. Adv.* **2014**, *32*, 462−484.
(31) McGillicuddy, N.; Floris, P.; Albrecht, S.; Bones, J. Examining the sources of variability in cell culture media used for biopharmaceutical production. *Biotechnol. Lett.* **2018**, *40*, 5−21.
(32) Gupta, A. J.; Gruppen, H.; Maes, D.; Boots, J.-W.; Wierenga, P. A. Factors Causing Compositional Changes in Soy Protein Hydrolysates and Effects on Cell Culture Functionality. *J. Agric. Food Chem.* **2013**, *61*, 10613−10625.
(33) Mackensen, A.; Dräger, R.; Schlesier, M.; Mertelsmann, R.; Lindemann, A. Presence of IgE antibodies to bovine serum albumin in a patient developing anaphylaxis after vaccination with human peptide-pulsed dendritic cells. *Cancer Immunol. Immunother.* **2000**, *49*, 152−156.
(34) Spees, J. L.; Gregory, C. A.; Singh, H.; Tucker, H. A.; Peister, A.; Lynch, P. J.; Hsu, S.-C.; Smith, J.; Prockop, D. J. Internalized Antigens Must Be Removed to Prepare Hypoimmunogenic Mesenchymal Stem Cells for Cell and Gene Therapy. *Mol. Ther.* **2004**, *9*, 747−756.
(35) Choi, S.; Murphy, W. L. Multifunctional Mixed SAMs That Promote Both Cell Adhesion and Noncovalent DNA Immobilization. *Langmuir* **2008**, *24*, 6873−6880.
(36) Chastain, S. R.; Kundu, A. K.; Dhar, S.; Calvert, J. W.; Putnam, A. J. Adhesion of mesenchymal stem cells to polymer scaffolds occurs via distinct ECM ligands and controls their osteogenic differentiation. *J. Biomed. Mater. Res., Part A* **2006**, *78A*, 73−85.
(37) Guo, M. L.; Chen, J. H.; Zhang, Y. J.; Chen, K.; Pan, C. F.; Yao, S. Z. Enhanced adhesion/spreading and proliferation of mammalian cells on electropolymerized porphyrin film for biosensing applications. *Biosens. Bioelectron.* **2008**, *23*, 865−871.
(38) Lahann, J.; Balcells, M.; Rodon, T.; Lee, J.; Choi, I. S.; Jensen, K. F.; Langer, R. Reactive polymer coatings: A platform for patterning proteins and mammalian cells onto a broad range of materials. *Langmuir* **2002**, *18*, 3632−3638.
(39) Bernards, M. T.; Cheng, G.; Zhang, Z.; Chen, S.; Jiang, S. Nonfouling Polymer Brushes via Surface-Initiated, Two-Component Atom Transfer Radical Polymerization. *Macromolecules* **2008**, *41*, 4216−4219.
(40) Tugulu, S.; Klok, H. A. Stability and nonfouling properties of poly(poly(ethylene glycol) methacrylate) brushes-under cell culture conditions. *Biomacromolecules* **2008**, *9*, 906−912.
(41) Lutolf, M. P.; Gilbert, P. M.; Blau, H. M. Designing materials to direct stem-cell fate. *Nature* **2009**, *462*, 433−441.
(42) Kloxin, A. M.; Kasko, A. M.; Salinas, C. N.; Anseth, K. S. Photodegradable Hydrogels for Dynamic Tuning of Physical and Chemical Properties. *Science* **2009**, *324*, 59−63.
(43) Qiu, Y.; Lim, J. J.; Scott, L., Jr.; Adams, R. C.; Bui, H. T.; Temenoff, J. S. PEG-based hydrogels with tunable degradation characteristics to control delivery of marrow stromal cells for tendon overuse injuries. *Acta Biomater.* **2011**, *7*, 959−966.
(44) Wilson, M. J.; Liliensiek, S. J.; Murphy, C. J.; Murphy, W. L.; Nealey, P. F. Hydrogels with well-defined peptide-hydrogel spacing and concentration: impact on epithelial cell behavior. *Soft Matter* **2012**, *8*, 390−398.
(45) DeForest, C. A.; Anseth, K. S. Advances in Bioactive Hydrogels to Probe and Direct Cell Fate. *Annu. Rev. Chem. Biomol. Eng.* **2012**, *3*, 421−444.
(46) Moreira, F.; Mizukami, A.; de Souza, L. E. B.; Cabral, J. M. S.; da Silva, C. L.; Covas, D. T.; Swiech, K. Successful Use of Human AB Serum to Support the Expansion of Adipose Tissue-Derived Mesenchymal Stem/Stromal Cell in a Microcarrier-Based Platform. *Front. Bioeng. Biotechnol.* **2020**, *8*, No. 594582.
(47) Tsai, A.-C.; Jeske, R.; Chen, X.; Yuan, X.; Li, Y. Influence of Microenvironment on Mesenchymal Stem Cell Therapeutic Potency: From Planar Culture to Microcarriers. *Front. Bioeng. Biotechnol.* **2020**, *8*, No. 640.
(48) Schmitt, S. K.; Murphy, W. L.; Gopalan, P. Crosslinked PEG mats for peptide immobilization and stem cell adhesion. *J. Mater. Chem. B* **2013**, *1*, 1349−1360.

https://dx.doi.org/10.1021/acsbiomaterials.0c00663
ACS Biomater. Sci. Eng. 2021, 7, 617−625

(49) Schmitt, S. K.; Xie, A. W.; Ghassemi, R. M.; Trebatoski, D. J.; Murphy, W. L.; Gopalan, P. Polyethylene Glycol Coatings on Plastic Substrates for Chemically Defined Stem Cell Culture. *Adv. Healthcare Mater.* **2015**, *4*, 1555−1564.
(50) Schmitt, S. K.; Trebatoski, D. J.; Krutty, J. D.; Xie, A. W.; Rollins, B.; Murphy, W. L.; Gopalan, P. Peptide Conjugation to a Polymer Coating via Native Chemical Ligation of Azlactones for Cell Culture. *Biomacromolecules* **2016**, *17*, 1040−1047.
(51) Krutty, J. D.; Dias, A. D.; Yun, J.; Murphy, W. L.; Gopalan, P. Synthetic, Chemically Defined Polymer-Coated Microcarriers for the Expansion of Human Mesenchymal Stem Cells. *Macromol. Biosci.* **2019**, *19*, No. 1800299.
(52) Corry, W. D. On the interaction of polystyrene latices and poly(l-lysine): II. Characterization of the particle-polymer System. *J. Colloid Interface Sci.* **1978**, *63*, 151−160.
(53) Mazia, D.; Schatten, G.; Sale, W. Adhesion of cells to surfaces coated with polylysine. Applications to electron microscopy. *J. Cell Biol.* **1975**, *66*, 198−200.
(54) Vroman, L. Effect of adsorbed proteins on the wettability of hydrophilic and hydrophobic solids. *Nature* **1962**, 476.
(55) Mbongue, J. C.; Nicholas, D. A.; Torrez, T. W.; Kim, N.-S.; Firek, A. F.; Langridge, W. H. R. The Role of Indoleamine 2, 3-Dioxygenase in Immune Suppression and Autoimmunity. *Vaccines* **2015**, *3*, 703−729.
(56) Ren, G.; Su, J.; Zhang, L.; Zhao, X.; Ling, W.; L'huillie, A.; Zhang, J.; Lu, Y.; Roberts, A. I.; Ji, W.; Zhang, H.; Rabson, A. B.; Shi, Y. Species Variation in the Mechanisms of Mesenchymal Stem Cell-Mediated Immunosuppression. *Stem Cells* **2009**, *27*, 1954−1962.
(57) Abdi, R.; Fiorina, P.; Adra, C. N.; Atkinson, M.; Sayegh, M. H. Immunomodulation by mesenchymal stem cells: a potential therapeutic strategy for type 1 diabetes. *Diabetes* **2008**, *57*, 1759−1767.
(58) Bartholomew, A.; Sturgeon, C.; Siatskas, M.; Ferrer, K.; McIntosh, K.; Patil, S.; Hardy, W.; Devine, S.; Ucker, D.; Deans, R.; Moseley, A.; Hoffman, R. Mesenchymal stem cells suppress lymphocyte proliferation in vitro and prolong skin graft survival in vivo. *Exp. Hematol.* **2002**, *30*, 42−48.
(59) Le Blanc, K.; Tammik, L.; Sundberg, B.; Haynesworth, S. E.; Ringdén, O. Mesenchymal Stem Cells Inhibit and Stimulate Mixed Lymphocyte Cultures and Mitogenic Responses Independently of the Major Histocompatibility Complex. *Scand. J. Immunol.* **2003**, *57*, 11−20.
(60) Leng, Z.; et al. Transplantation of ACE2$^-$ Mesenchymal Stem Cells Improves the Outcome of Patients with COVID-19 Pneumonia. *Aging Dis.* **2020**, *11*, 216−228.
(61) Belair, D. G.; Khalil, A. S.; Miller, M. J.; Murphy, W. L. Serum-Dependence of Affinity-Mediated VEGF Release from Biomimetic Microspheres. *Biomacromolecules* **2014**, *15*, 2038−2048.
(62) Belair, D. G.; Murphy, W. L. Specific VEGF sequestering to biomaterials: Influence of serum stability. *Acta Biomater.* **2013**, *9*, 8823−8831.
(63) Zhu, X. D.; Fan, H. S.; Xiao, Y. M.; Li, D. X.; Zhang, H. J.; Luxbacher, T.; Zhang, X. D. Effect of surface structure on protein adsorption to biphasic calcium-phosphate ceramics in vitro and in vivo. *Acta Biomater.* **2009**, *5*, 1311−1318.
(64) Simaria, A. S.; Hassan, S.; Varadaraju, H.; Rowley, J.; Warren, K.; Vanek, P.; Farid, S. S. Allogeneic cell therapy bioprocess economics and optimization: Single-use cell expansion technologies. *Biotechnol. Bioeng.* **2014**, *111*, 69−83.

https://dx.doi.org/10.1021/acsbiomaterials.0c00663
ACS Biomater. Sci. Eng. 2021, 7, 617−625